



VICTORIA UNIVERSITY
MELBOURNE AUSTRALIA

Loss of endogenous estrogen alters mitochondrial metabolism and muscle clock-related protein Rbm20 in female mdx mice

This is the Published version of the following publication

Timpani, Cara, Debrincat, Didier, Kourakis, Stephanie, Boyer, Rebecca, Formosa, Luke E, Steele, Joel R, Zhang, Haijian, Schittenhelm, Ralf B, Russell, Aaron P, Rybalka, Emma and Lindsay, Angus (2024) Loss of endogenous estrogen alters mitochondrial metabolism and muscle clock-related protein Rbm20 in female mdx mice. *FASEB journal : official publication of the Federation of American Societies for Experimental Biology*, 38 (11). e23718. ISSN 0892-6638

The publisher's official version can be found at
<http://dx.doi.org/10.1096/fj.202400329r>
Note that access to this version may require subscription.

Downloaded from VU Research Repository <https://vuir.vu.edu.au/48151/>

RESEARCH ARTICLE

Loss of endogenous estrogen alters mitochondrial metabolism and muscle clock-related protein Rbm20 in female *mdx* mice

Cara A. Timpani^{1,2,3}  | Didier Debrincat⁴  | Stephanie Kourakis^{1,2}  |
Rebecca Boyer⁴ | Luke E. Formosa⁵  | Joel R. Steele⁶  | Haijian Zhang⁶  |
Ralf B. Schittenhelm⁶  | Aaron P. Russell⁷  |
Emma Rybalka^{1,2,3,8}  | Angus Lindsay^{7,9,10} 

¹Institute for Health and Sport (IHES), Victoria University, Melbourne, Victoria, Australia

²Inherited and Acquired Myopathies Program, Australian Institute for Musculoskeletal Science (AIMSS), St Albans, Victoria, Australia

³Department of Medicine—Western Health, Melbourne Medical School, The University of Melbourne, St Albans, Victoria, Australia

⁴College of Health and Biomedicine, Victoria University, Melbourne, Victoria, Australia

⁵Department of Biochemistry and Molecular Biology, Monash Biomedicine Discovery Institute, Monash University, Clayton, Victoria, Australia

⁶Monash Proteomics and Metabolomics Platform, Department of Biochemistry and Molecular Biology, Monash University, Clayton, Victoria, Australia

⁷Institute for Physical Activity and Nutrition, School of Exercise and Nutrition Sciences, Deakin University, Geelong, Victoria, Australia

⁸Division of Neuropaediatrics and Developmental Medicine, University Children's Hospital of Basel (UKBB), Basel, Switzerland

⁹School of Biological Sciences, University of Canterbury, Christchurch, New Zealand

¹⁰Department of Medicine, University of Otago, Christchurch, New Zealand

Correspondence

Emma Rybalka, Institute for Health and Sport, Victoria University, PO Box 14428, Melbourne, VIC 8001, Australia.

Email: emma.rybalka@vu.edu.au

Angus Lindsay, School of Biological Sciences, University of Canterbury, Christchurch 8041, New Zealand.

Email: angus.lindsay@canterbury.ac.nz

Funding information

Deakin University; Deakin University | Institute for Physical Activity and Nutrition (IPAN); Neurological Foundation of New Zealand; Manatu Hauora | Health Research Council of New Zealand (HRC); DHAC | National Health and Medical Research Council (NHMRC), Grant/Award Number:

Abstract

Female carriers of a *Duchenne muscular dystrophy* (*DMD*) gene mutation manifest exercise intolerance and metabolic anomalies that may be exacerbated following menopause due to the loss of estrogen, a known regulator of skeletal muscle function and metabolism. Here, we studied the impact of estrogen depletion (via ovariectomy) on exercise tolerance and muscle mitochondrial metabolism in female *mdx* mice and the potential of estrogen replacement therapy (using estradiol) to protect against functional and metabolic perturbations. We also investigated the effect of estrogen depletion, and replacement, on the skeletal muscle proteome through an untargeted proteomic approach with TMT-labelling. Our study confirms that loss of estrogen in female *mdx* mice reduces exercise capacity, tricarboxylic acid cycle intermediates, and citrate synthase activity but that these deficits are offset through estrogen replacement therapy. Furthermore, ovariectomy downregulated protein expression of RNA-binding motif factor 20 (Rbm20), a critical regulator of sarcomeric and muscle homeostasis gene splicing, which impacted pathways involving

This is an open access article under the terms of the [Creative Commons Attribution](https://creativecommons.org/licenses/by/4.0/) License, which permits use, distribution and reproduction in any medium, provided the original work is properly cited.

© 2024 The Author(s). *The FASEB Journal* published by Wiley Periodicals LLC on behalf of Federation of American Societies for Experimental Biology.

ribosomal and mitochondrial translation. Estrogen replacement modulated Rbm20 protein expression and promoted metabolic processes and the upregulation of proteins involved in mitochondrial dynamics and metabolism. Our data suggest that estrogen mitigates dystrophinopathic features in female *mdx* mice and that estrogen replacement may be a potential therapy for post-menopausal DMD carriers.

KEYWORDS

Duchenne muscular dystrophy, dystrophin, estrogen, metabolism, metabolomics, mitochondria, molecular clock, proteomics, Rbm20, skeletal muscle

1 | INTRODUCTION

Metabolic and mitochondrial dysfunction is a well-established nuance of dystrophin-deficient skeletal muscle.^{1–6} Mutation of the X-chromosome residing *DMD* gene that leads to the loss of the cytoskeletal dystrophin protein, causes Duchenne muscular dystrophy (DMD), a progressive and eventually fatal neuromuscular disease that predominantly affects males. Loss of control of several metabolic systems, for example, mitochondrial tricarboxylic acid (TCA) cycle and electron transport chain (ETC) function, glycolysis, and purine nucleotide metabolism, perpetuates the DMD pathobiology by compromising cellular energy homeostasis and promoting oxidative stress.¹ However, the root cause of these metabolic disturbances is unclear. Some purported theories include (1) loss of nitric oxide synthesis due to deficient dystrophin-neuronal NO synthase (nNOS) binding⁷; (2) loss of calcium homeostasis owing to enhanced sarcolemmal fragility and calcium leak channel hyperactivity caused by dystrophin deficiency resulting in persistent induction of the mitochondrial permeability transition pore⁸; (3) dysregulated purine nucleotide cycle function leading to purine degradation and reduced ATP recovery potential⁹; (4) upregulated micro RNA (miR)-379, resulting in reduced mitochondrial ATP synthase function¹⁰; and (5) dysregulated mitophagy and mitobiogenesis signalling.¹¹ Mitochondrial and metabolic dysfunction is evident in dystrophic myoblasts¹² and early in the pathological dystrophinopathy milieu leading to muscle degeneration.¹³ Targeting mitochondria/metabolism can ameliorate disease pathology in the *mdx* mouse model of DMD, for example, via mitochondria transplantation¹⁴ or targeted drug therapies (ginovistat targets HDACs,¹⁵ urolithin A activates mitophagy,¹¹ and dimethyl fumarate targets TCA anaplerosis¹⁶).

In addition to DMD patients and animal models that carry biallelic *DMD/Dmd* gene mutations, mitochondrial/metabolic dysfunction is evident in female carriers of a DMD gene mutation. Approximately two-thirds of DMD patients inherit mutations from carrier mothers (the other one-third of cases occur due to de novo mutation¹⁷).

These carriers frequently report exercise intolerance, being unable to perform the same extent of muscle work for a matched workload as non-carriers.^{18,19} They also take longer to recover high phosphate energy stores post-exercise^{18,19} and show sharp increases in serum CK,²⁰ suggesting susceptibility of muscle fibers to mechanical damage even though dystrophin is expressed (albeit sub-optimally²¹). However, rarely do they manifest progressive muscle wasting (<10% of cases).²² Female DMD carriers might be particularly susceptible to manifestations of DMD as they reach menopause and the protective effects of endogenous estrogen production subside. Indeed, several case studies highlight muscle wasting and pathology causing disability in ~50-year-old DMD carriers.^{23,24}

The *mdx* mouse model of DMD carries a point mutation in the *DMD* gene and shows various degrees of metabolic perturbation despite an overall milder phenotype than DMD patients. Both male and female mice carry the biallelic gene mutation due to inbreeding and share natural history homology except that females are more resistant to laboratory-based stressors (e.g., handling and scruffing^{25,26}). To explore this aspect further, we recently assessed the phenotype in ovariectomized female *mdx* mice to test the hypothesis that estrogen was protective against heightened stress responses.^{25,26} Although estrogen depletion did not exacerbate the muscle-specific phenotype, our serum metabolomics screen indicated that mitochondrial TCA cycle metabolite levels were reduced but were effectively replenished by estradiol (E2) therapy.²⁶ The protective effects of estrogen on skeletal and cardiac muscle have been demonstrated previously,²⁷ but never linked to metabolic dysfunction in the context of dystrophin deficiency. Pharmacological estrogen receptor modulation has been pursued as a potential therapy for DMD. The selective estrogen receptor alpha (ER α) agonist, tamoxifen, was initially shown in *mdx* mice to improve whole-body strength and skeletal muscle function, and reduce cardiac pathology.²⁸ More recent work demonstrates that it lessens contractile dysfunction in stem-cell-derived cardiomyocytes.²⁹ However, clinical trials in Switzerland could not show that tamoxifen modified

the natural history of DMD progression despite improvements in some functional measures.^{30,31} The potential of ER α modulation may not be fully realized in male patients who express fewer ERs than female counterparts, but it could be useful to protect female carriers from progressive disease in the peri-/menopausal years.

The aim of this study was to explore the impact of estrogen depletion on muscle mitochondrial metabolism and the potential for E2 replacement therapy to protect against metabolic maladaptation in female *mdx* mice. We studied the effect of estrogen manipulation on the skeletal muscle proteome using an untargeted proteomic approach with TMT-labelling and demonstrated that estrogen depletion alters mitochondrial metabolism and the muscle clock-related protein,³² RNA-binding motif factor 20 (Rbm20).

2 | MATERIALS AND METHODS

2.1 | Study approval

This research was approved by the Deakin University Animal Ethics Committee (G09-2020). Mice used in this study were housed in accordance with the Deakin University Animal Welfare Committee standards and cared for in accordance with the Australian Code for Care and Use of Animals for Scientific Purposes.

2.2 | Experimental design and animals

Muscles analyzed in this study were collected from mice utilized in Lindsay *et al.*^{25,26} Briefly, 8-week-old C57BL/10ScSn-*Dmd*^{*mdx*}/Arc female mice (homozygous) subjected to a sham surgery, ovariectomy (OVX) or OVX+E2 supplementation, and were purchased from ARC (Western Australia, Australia; *n* = 15/group). Mice underwent surgery in which the ovary and oviduct was exteriorized and either returned into the peritoneal cavity (Sham) or cauterized between the uterine horn and oviduct (OVX and OVX+E2). Once the muscle wall was closed, either a placebo (Sham and OVX) or E2 pellet (OVX+E2; 3.4 μ g/day E2 release) was inserted under the skin. Mice recovered for 2 weeks prior to shipment to Deakin University. All mice were housed in groups of four/cage on a 12/12h light/dark cycle with food and water provided ad libitum. Mice acclimatized for 1 week before undergoing scruff restraint. A forced downhill treadmill exercise-to-fatigue test was performed where the treadmill was set at 0 m/min for 2 min before increasing to 10 m/min for 1 min. The treadmill speed increased by 1 m/min until a speed of 15 m/min was reached and then maintained for 15 min. A second scruff restraint was

performed 1 week later and 15 min after the final scruff restraint, mice were sacrificed via CO₂ asphyxiation and cervical dislocation. Blood was collected, and muscles were harvested, snap-frozen, and stored at -80°C until required. Estrogen depletion via OVX and repletion via E2 were confirmed through measurement of the uterine mass, a reliable surrogate measure of circulating estrogen levels.^{33,34}

2.3 | Metabolomics

Metabolomics was performed in Lindsay and Russell 2023.²⁵ Briefly, serum samples were extracted using a 1:1 acetonitrile/methanol solution, vortexed, incubated at 4°C for 10 min and centrifuged at 4°C for 10 min on maximum speed (20800g). The supernatant was transferred into a HPLC insert and the polar metabolites were separated and analyzed via mass spectrometry at Metabolomics Australia (Bio21 Molecular Science and Biotechnology Institute, University of Melbourne, Parkville, Australia).

2.4 | Muscle oxidative capacity

OCT-covered gastrocnemius, tibialis anterior (TA) and diaphragm muscles were cryo-sectioned (10 μm at -15°C) and succinate dehydrogenase (SDH) capacity was quantified as described by us previously.^{16,35}

2.5 | Mitochondrial enzyme activity

Activity of citrate synthase (CS), an enzyme of the TCA cycle, was measured spectrophotometrically in gastrocnemius homogenates as described by us previously.^{16,35} To complement assessment of SDH activity in muscle sections, activity of SDH/mitochondrial ETC complex II (CII) was assessed on isolated mitochondria from gastrocnemius muscles according to the manufacturer directions (Abcam, ab228560). Mitochondria were isolated as performed by us previously.³⁶

2.6 | Proteomics

2.6.1 | Protein extraction from samples and enzymatic digestion

Quadriceps were cryo-pulverized with subsequent solubilization in 5% sodium dodecyl sulfate (SDS) 10 mM Tris HCl, heat inactivation performed at 95°C for 10 min followed by probe sonication 3×30 s rounds and centrifuged

at 13 000 g for 5 min to clarify. The supernatant of each sample was transferred to a new tube, and protein concentration was measured using a BCA kit (Thermo Fisher, #23225) according to the manufacturer's instructions. Samples were then processed using the S-trap protocol as per the manufacturer's instructions (Protifi³⁷). Normalized amounts of protein were reduced and alkylated with 10 mM TCEP (Thermo, #77720) and 40 mM chloroacetamide (Sigma, C0267-100G) with incubation at 55°C for 15 min. Enzymatic digestion was performed using Trypsin (Promega, V528X) at a 1:50 wt:wt ratio alongside Lys-C at a 1:25 wt:wt ratio (Promega, VA1170) at 37°C for 16 h. Digestion efficiency was greater than 94% for this analysis.

2.6.2 | Tandem mass tag (TMT) labelling and fractionation

Each sample was labeled with the TMTpro 18plex reagent set (Lot: XJ351218 and XK350589, Thermo Scientific) according to the manufacturer's instructions utilizing a singular reference channel (126) containing all samples pooled. Individual labeled samples were then pooled into plexes, and high-pH RP-HPLC was used to generate 36 fractions concatenated to 12, which have been acquired individually by LC-MS/MS to maximize identifications. Labelling efficiency was determined to be greater than 97%.

2.6.3 | Liquid chromatography mass spectrometry protocol

Liquid chromatography-mass spectrometric (LC-MS) analysis was conducted using an Orbitrap Eclipse Tribrid mass spectrometer (Thermo Scientific, Bremen, Germany) and Nano LC system (Dionex Ultimate 3000 RSLCnano). The samples were loaded onto an Acclaim PepMap 100 trap column (100 $\mu\text{m} \times 2\text{ cm}$, nanoViper, C18, 5 μm , 100 \AA ; Thermo Scientific) and separated on an Acclaim PepMap RSLC (75 $\mu\text{m} \times 50\text{ cm}$, nanoViper, C18, 2 μm , 100 \AA ; Thermo Scientific) analytical column. The peptides were resolved by increasing concentrations of buffer B (80% acetonitrile/0.1% formic acid) and analyzed via 2 kV nano-electrospray ionization. The mass spectrometer operated in data-dependent acquisition mode using in-house optimized parameters with 120 min of chromatographic separation used for each fraction. Briefly, the acquisition used three FAIMS compensation voltages (-40, -55, -70 V) operated under standard resolution with an ion transfer tube temperature of 300°C with a carrier gas flow rate of 4.6 L/min. Precursor ion scans were performed at a 120 000 resolution from 400 to 1600 m/z, an AGC target of 250% and ion injection time

set to auto. Peptide fragmentation and reporter tag quantification were performed synchronously (10 per duty cycle per compensation voltage) with the fragmentation spectra generated in the ion trap using CID with turbo scan rate; MS3 reporter ion measurements were performed in the orbitrap with a resolution of 50 000. A precursor isolation filter was used for the selection of ions with a 0.7 Da and 50% envelope fit. Dynamic exclusion was applied for 60 s across all compensation voltages with only one charge state per precursor selected for fragmentation. In addition, the use of real-time searching was performed with a close out of 10 peptides per protein within each injected fraction; this utilized the human SwissProt proteome with 1% false discovery filtering applied during acquisition.

2.6.4 | Mass spectrometric data analysis

The raw data files were analyzed using Sequest within Proteome Discoverer (v2.5.0.400, Thermo Scientific) to obtain protein identifications and their respective reporter ion intensities using in-house standard parameters. The Mouse SwissProt proteome containing only reviewed sequences (accessed June 2023) was used for protein identification at a 1% false discovery rate (FDR) alongside a common contaminants database. Reporter ion quantifiers used a unique plus razor with analysis centered on protein groups for shared peptide sequences using all peptides for abundance determination; quantitative values were corrected for stable isotope label impurities according to the manufacturer's values.

2.6.5 | Bioinformatic data analysis

Protein level data were exported and analyzed utilizing TMT-Analyst, the latest addition to the Monash Proteomic Analyst Suite (<https://analyst-suites.org/>), which is built upon the foundations of LFQ-Analyst.^{38,39} Briefly, prior to normalization, proteomic data were filtered for high-confidence proteins from already determined master proteins representing groups. Proteins marked as contaminants and proteins not quantified consistently (condition $N/2 + 1$) across the experiment were removed. The remaining missing values were imputed using the missing-not-at-random (MNAR) method, assuming the missingness was due to low expression for such proteins, which were then normalized using the variance-stabilizing-normalization (VSN) method. Both imputations and VSN were conducted by the DEP package.⁴⁰ The limma package⁴¹ from R Bioconductor was used to generate a list of differentially expressed proteins for each pair-wise comparison. A cut-off of the adjusted *p*-value of 0.05 (Benjamini-Hochberg method) and a log₂ fold change of 0.75 was applied to

determine significantly regulated proteins in the different pairwise comparisons. We utilized the protein abundance data obtained from the LFQ-Analyst suite and conducted differential pathway analysis using Correlation Adjusted MEan RAnk gene set test (CAMERA)-intensity based analysis within Reactome (v83).⁴² Briefly, this method uses limma-based differential analysis on mean protein abundances within pathways across samples with adjusted FDR correction to control for multiple hypothesis testing. Using this approach enables the detection of alterations in pathways that will likely remain unobserved when examining individual differentially expressed proteins. This is because individual proteins might not provide comprehensive insights into how a specific pathway is changing when assessed through global, untargeted proteomic-level statistical comparisons. The FDR of <0.05 is reported.

2.7 | Statistics

Data are reported as mean \pm SEM unless stated otherwise. Normal distribution of the data was assessed using a Shapiro–Wilk test and all data passed the normality test except for the forced downhill treadmill exercise-to-fatigue test. These data were analyzed using a Kruskal–Wallis test and a Dunn's multiple comparison test was performed post hoc. All other data, excluding proteomics (see section 2.6.5), were analyzed using one-way ANOVA with Tukey's post hoc test on GraphPad Prism version 10.0.3 (GraphPad Software, Boston, Massachusetts, USA). α was set at .05 and trends are reported at <.1.

3 | RESULTS

3.1 | Estrogen replacement therapy recovers exercise capacity and mitochondrial metabolism

The impact of estrogen depletion on exercise capacity of female *mdx* mice was assessed via a forced downhill treadmill exercise-to-fatigue test. OVX reduced the exercise capacity of female *mdx* mice by ~64% compared to Sham (Figure 1A; $p < .0001$) with E2 replacement normalizing exercise capacity to Sham levels (~133% increase, Figure 1A; $p < .01$). Since exercise capacity is intricately linked to mitochondrial metabolism, the metabolomics data set was analyzed to assess TCA cycle intermediates. Metabolomic analysis captured six of nine TCA cycle intermediates, and when pooled, OVX reduced TCA metabolite content compared to Sham (Figure 1B; $p < .0001$). This main effect was mostly accounted for by reduced cis-aconitate (biggest

reduction, reduced by 40% from Sham, $p < .05$) and succinate (most significant reduction, reduced by 30% from Sham, $p < .0001$) (Figure 1C). As with exercise capacity, E2 replacement therapy restored the TCA metabolite pool (Figure 1B; $p < .05$), especially succinate concentration (restored to 92% of Sham, Figure 1C; $p < .05$).

3.2 | Estrogen replacement recovers mitochondrial content in gastrocnemius but reduces SDH capacity in TA and diaphragm

Since OVX affected mitochondria-specific metabolic intermediates, the activity of key mitochondrial enzymes was determined, including (1) CS, the pace setter of TCA cycle flux and a well-established biomarker of mitochondrial content, and (2) SDH, which couples TCA cycle flux to ETC function. Since metabolic intermediates were quantified in serum, it was necessary to confirm alterations in muscle mitochondrial enzyme activity were associated with the serum metabolic signature as was shown previously.⁴³ CS activity of whole muscle homogenates was reduced in OVX compared to Sham gastrocnemius (Figure 2A; $p < .01$) and was recovered via E2 replacement (Figure 2A; $p < .0001$), indicative of either increased substrate flux or mitochondrial density. Despite an ~40% reduction in mean values, there was no statistically significant effect of OVX on SDH activity of isolated mitochondria from the gastrocnemius (Figure 2B; $p = .6491$). There was, however, a trend for E2 replacement to increase SDH activity compared to OVX mice (Figure 2B; $p = .0898$). SDH capacity of the gastrocnemius was also assessed through histological staining to provide information on potential fiber type shifts (Figure 2C; $p > .05$). SDH capacity of two other muscles – one being the TA, which is commonly analyzed for histology, and the diaphragm, which is typically impacted as the dystrophic disease worsens, were also assessed. Interestingly, OVX significantly increased the SDH capacity of TA (Figure 2D; $p < .01$) and trended to do the same in the diaphragm (Figure 2E; $p = .0691$). In both muscles, E2 replacement normalized SDH capacity to Sham levels (Figure 2D,E, respectively; $p < .01$). While the proportion of less, more, and highly oxidative fibers did not shift in the gastrocnemius (Figure 2F and Figure S1A^{I–III}; $p > .05$), OVX drove a less oxidative phenotype in the fast-twitch fiber predominant TA (Figure 2G and Figure S1B^{I–III}; $p < .01$), which was normalized by E2 replacement (Figure 2G and Figure S1B^{I–III}; $p < .01$). In contrast, OVX increased the proportion of more oxidative fibers in the diaphragm compared to Sham (Figure 2H and Figure S1C^{II}; $p < .05$) while E2 replacement tended to increase the proportion of highly oxidative fibers in OVX diaphragm (Figure 2H and Figure S1C^{III}; $p = .086$).

3.3 | Estrogen depletion downregulates the protein expression of Rbm20, which is normalized by estrogen replacement and upregulates metabolic proteins

E2 replacement recovered both exercise capacity and CS activity. Therefore, the effect of OVX, and subsequently E2 replacement, on proteins involved in metabolism were investigated. To address this with an unbiased method, we performed TMT labelling of muscle lysates following trypsin and Lys-C digestion and subjected these to LC-MS analysis. More than 5400 distinct proteins were identified by untargeted, label-based proteomics using TMT and interestingly, only one protein, Rbm20, was found to be significantly regulated using a \log_2 fold change cutoff of 0.75 and an adjusted p value of <0.05 . Rbm20 (accession Q3UQS8), which regulates post-transcriptional splicing of sarcomeric and other muscle homeostasis genes, was downregulated in OVX compared to Sham muscle (Figure 3A,A¹; $p < .0001$). To understand whether OVX impacts families of proteins, which were not detected as significant due to the \log_2 fold change cutoff and p value criteria, pathway analysis (via Reactome) of the entire proteome dataset was conducted.⁴⁴ A total of 59 pathways were impacted by OVX (Figure 3B). Sixteen pathways were upregulated after OVX and particularly involved processes associated with vision (e.g., retinoid metabolism and transport, visual phototransduction, diseases associated with visual transduction, the canonical retinoid cycle in rods (twilight vision)). Of the 43 pathways that were downregulated following OVX, a significant proportion were associated with translational activity (e.g., eukaryotic translation initiation and elongation, cap-dependent translation initiation, mitochondrial translation). Restoration of estrogen through E2 replacement led to the significant upregulation of the Rbm20 protein (compared to OVX; Figure 4A,A¹) as well as the modulation of a further 61 proteins, upregulating 29 and downregulating 32. Since Rbm20 was impacted by both OVX and E2 replacement, we probed the proteome dataset for its splicing targets⁴⁵ to determine if the down- and upregulation of Rbm20 impacted subtle, but biologically relevant, changes on downstream proteins. Of the 30 proteins captured in our proteomics set, three proteins were downregulated following OVX (Camk2d and Pdlim3 ($p < .05$) and Dtna ($p < .01$); Figure 4B) and one protein was upregulated (Myh7, $p < .05$). E2 replacement upregulated the expression of five proteins (Camk2d and Pdlim5 ($p < .05$), Dtna ($p < .01$) and Mlip and Sh3kbp1 ($p < .0001$)) and downregulated the expression of two proteins (Nexn ($p < .05$) and Mecp2 ($p < .001$)).

Of the 29 proteins that were upregulated by E2 replacement, a critical protein associated with orchestrating metabolic flux between the cytosolic glycolytic pathway and the mitochondrial TCA cycle, pyruvate carboxylase (Pc), was

upregulated indicating a mechanism for the metabolomic shift. Indeed, pathways analysis revealed that of the 88 pathways modulated by E2 replacement (34 upregulated and 54 downregulated), key metabolic processes were upregulated, including the TCA cycle and respiratory ETC (Figure 4C). Furthermore, mitochondrial processes, including translation and import, were upregulated, suggesting an overall increase in mitochondrial activity. This motivated us to probe the proteomics dataset for key proteins driving these changes. Several proteins in the large and small subunit of the mitoribosome were downregulated by OVX (Mrpl12, Mrpl14, Mrpl20, Mrpl32, Mrpl50, Mrps28, and Mrps34, $p < .05$, Figure 5A) with E2 replacement upregulating the expression of six large subunit proteins ($p < .05$) and 17 small subunit proteins ($p < .05$ –.0001). Markers of mitochondrial dynamics, including Cs, Mfn1 and Mfn2 (mitofusins), Opa1 (optic atrophy 1), Perm1 (PGC-1/ERR-induced regulator in muscle 1), Tfam (mitochondrial transcription factor A), and Vdac 1–3 (voltage-dependent anion channel), were not affected by OVX (Figure 5B; $p > .05$) but Mfn1, Perm1, Tfam, and Vdac2 ($p < .01$) were significantly increased by E2 replacement. Notably, Cs protein expression was unaffected indicating estrogen-mediated changes in activity are not due to reduced mitochondrial mass/density. To assess secondary mitochondrial control mechanisms, we probed proteins associated with calcium metabolism (calcium allosterically regulates TCA cycle dehydrogenases, Figure S2A) and mitochondrial uncoupling (which can deplete the mitochondrial membrane potential, Figure S2B). Atp2a2 was the only protein associated with calcium metabolism to be upregulated following OVX ($p < .01$) while Camk2d, Mcu, Micu2, Saraf ($p < .05$), and Micu1 ($p < .01$) were downregulated. E2 replacement downregulated six proteins, including Ryr1 ($p < .05$ –.001) and upregulated the expression of four proteins including mitochondrial calcium uptake proteins, Micu 1 and 2 ($p < .01$ –.0001). Only one protein, Mcu, which is associated with both calcium homeostasis and the mitochondrial membrane potential, was downregulated following OVX ($p < .05$). Vdac2 ($p < .01$) and Mcu ($p < .0001$) were both upregulated with E2 replacement. These data suggest estrogen may be important for controlling mitochondrial calcium uptake and calcium-mediated control of mitochondrial ATP production rate.

Since Pc was significantly upregulated following E2 replacement (Figure 4A,A¹), proteins associated with pyruvate metabolism were explored. While it was not detected as a significantly dysregulated protein based on the \log_2 fold change criteria of 0.75 (Figure 3A), loss of estrogen downregulated the expression of Pc in OVX mice compared to Sham (Figure 5C; $p < .001$). OVX had no impact on any of the other 11 proteins associated with pyruvate metabolism ($p > .05$). However, E2 replacement upregulated expression of Pdp1 (pyruvate dehydrogenase phosphatase 1) and Pdpr (pyruvate dehydrogenase phosphatase

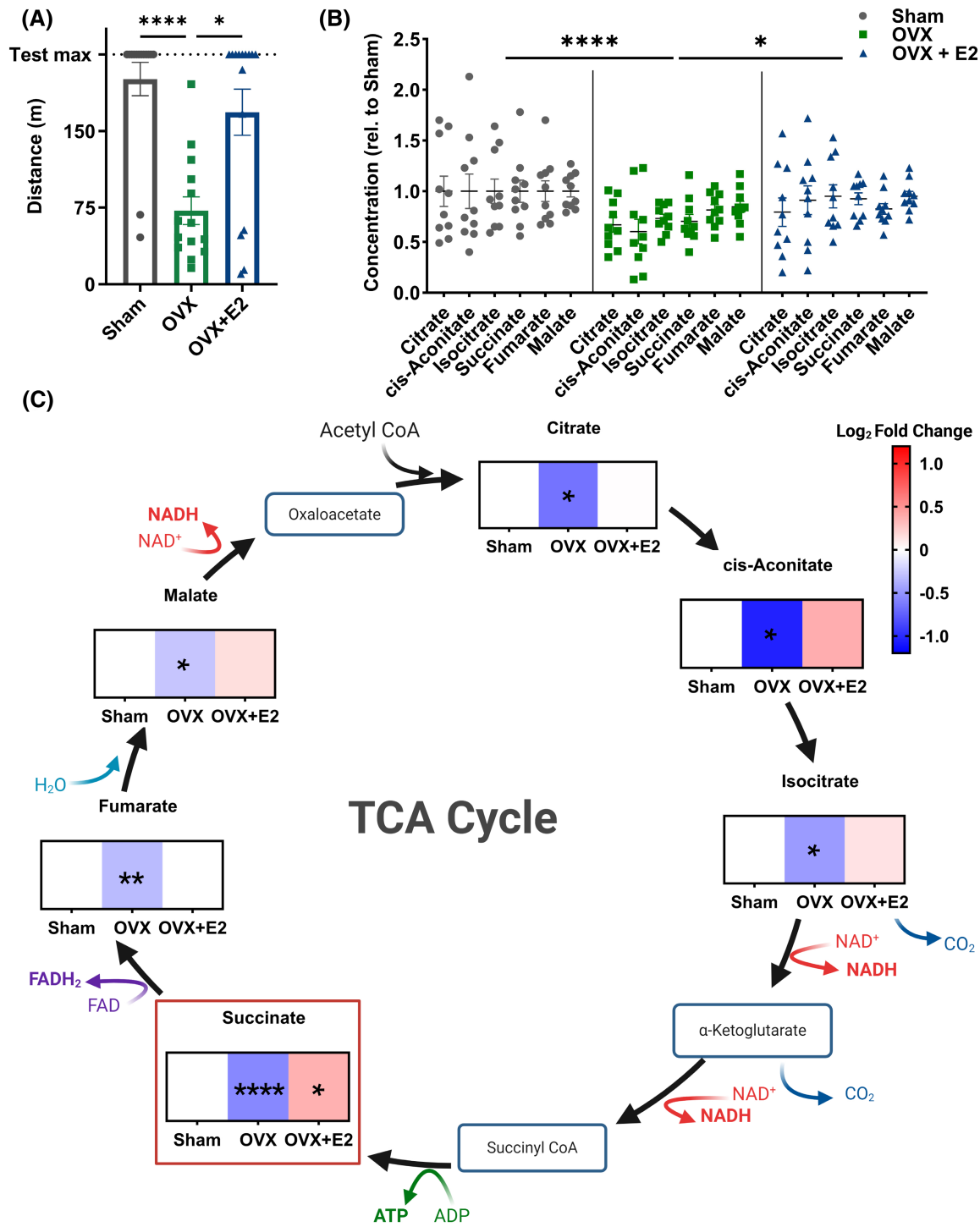


FIGURE 1 Estrogen depletion reduces exercise capacity and mitochondrial metabolism intermediates in female *mdx* mice that can be recovered with estradiol (E2) replacement. (A) Exercise capacity, as assessed by a forced downhill treadmill exercise-to-fatigue test, was reduced in ovariectomized (OVX) mice compared to Sham with E2 replacement improving exercise capacity in OVX mice. (B) Concentration of pooled tricarboxylic acid (TCA) cycle intermediates is reduced following OVX but is restored after E2 replacement therapy. (C) The reduction in pooled TCA cycle intermediates was driven by a significant decrease in cis-aconitate and succinate concentration and succinate concentration was recovered with E2 replacement. Data in (C) is expressed as the log₂ fold change. * $p < .05$; ** $p < .01$; **** $p < .0001$. Sham $n = 10-14$; OVX $n = 10-14$; OVX + E2 $n = 10-15$.

regulatory subunit) compared to OVX mice ($p < .05$). We next assessed proteins of the TCA cycle since we observed an increase in TCA cycle intermediates (Figure 1B-D) and

CS activity (Figure 2A) following E2 replacement. Of the proteins captured in this dataset, OVX increased the expression of isocitrate dehydrogenase 2 (*Idh2*; Figure 5D;

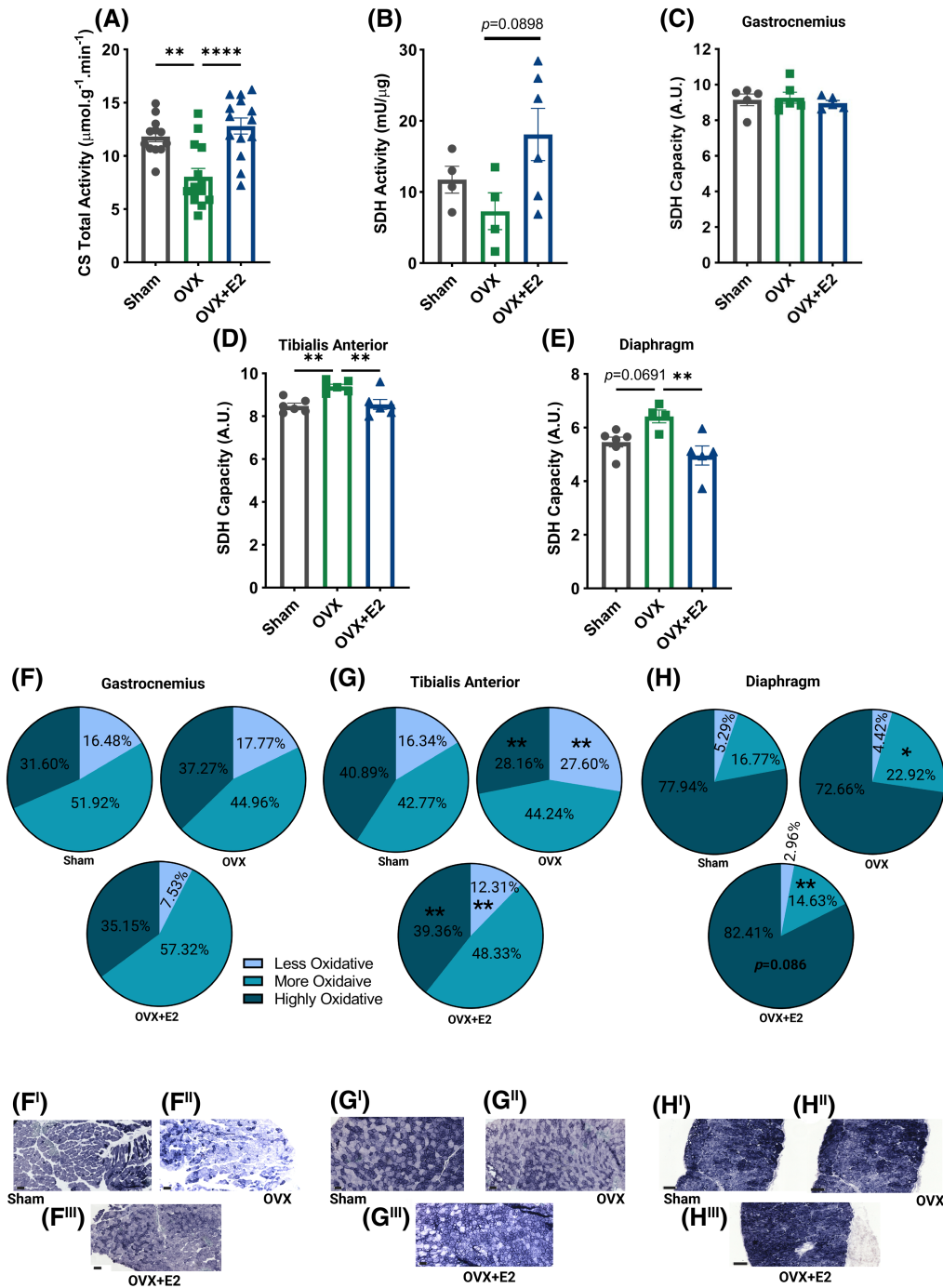


FIGURE 2 Estrogen depletion reduces citrate synthase (CS) but not succinate dehydrogenase (SDH) activity in gastrocnemius of female *mdx* mice. (A) CS activity, a surrogate for mitochondrial content, was reduced in ovariectomized (OVX) gastrocnemius compared to Sham, which was recovered with estradiol (E2) replacement. (B) While SDH enzyme activity was comparable between Sham and OVX mitochondria isolated from gastrocnemius, there was a trend for E2 replacement to increase SDH activity ($p = .0898$). Using SDH histological staining of muscle sections, SDH capacity of gastrocnemius was comparable across all groups (Sham, OVX and OVX + E2; C), but was increased in tibialis anterior (D), with a trend detected in diaphragm ($p = .0691$; E), following OVX. In both tibialis anterior and diaphragm, E2 replacement decreased the SDH capacity (D and E). (F-H) The proportion of less, more, and highly oxidative fibers is shown for gastrocnemius, tibialis anterior and diaphragm with representative images (F-H'''). * $p < .05$; ** $p < .01$; **** $p < .0001$. Sham $n = 5-12$; OVX $n = 4-14$; OVX + E2 $n = 5-14$. Scale bar = 100 μm .

$p < .01$) and a component of the SDH complex (Sdhb; $p < .05$) compared to Sham. While E2 replacement was unable to modulate Sdhb expression ($p > .05$), it reduced

the expression of Idh2 ($p < .0001$). Since pathway analysis revealed the ETC as an upregulated process, we next evaluated proteins associated with each respiratory complex

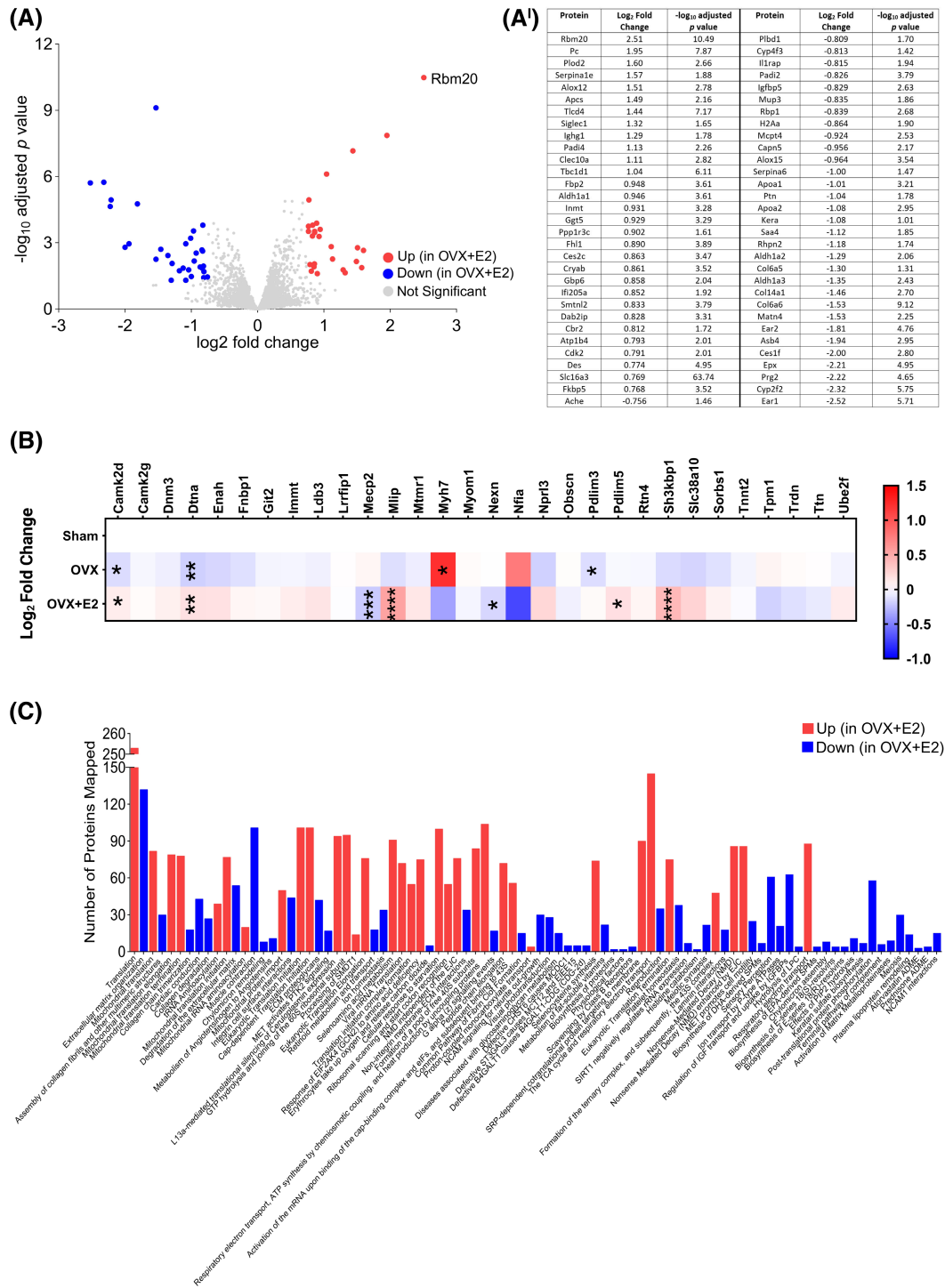


FIGURE 4 Estrogen replacement upregulates Rbm20 expression in female *mdx* mice and modulates the expression of a further 61 proteins. (A and A¹) Rbm20 expression was upregulated following estradiol (E2) replacement as well as modulated expression of a further 61 others. (B) The impact of ovariectomy (OVX) and E2 replacement, is demonstrated on splicing targets of Rbm20. (C) Pathways analysis of the entire proteomics dataset identified that 88 pathways were impacted by E2 replacement – 34 pathways were upregulated compared to OVX muscle while 54 pathways were downregulated. Order of pathways is presented as most significantly impacted (i.e., translation) to least significantly impacted (i.e., NCAM1 interactions). * $p < .05$; ** $p < .01$; *** $p < .001$; **** $p < .0001$. OVX versus Sham $n = 5$; OVX $n = 6$; OVX + E2 versus OVX. Sham $n = 5$; OVX $n = 6$; OVX + E2 $n = 6$.

normalized its expression ($p < .05$). E2 replacement also upregulated the expression of the CV subunits Atp5mg, Atp5po ($p < .05$), and Atpaf2 ($p < .01$).

To further explore the relationship between Rbm20 expression and changes to key metabolic indices and proteins, we conducted correlation and regression analyses.

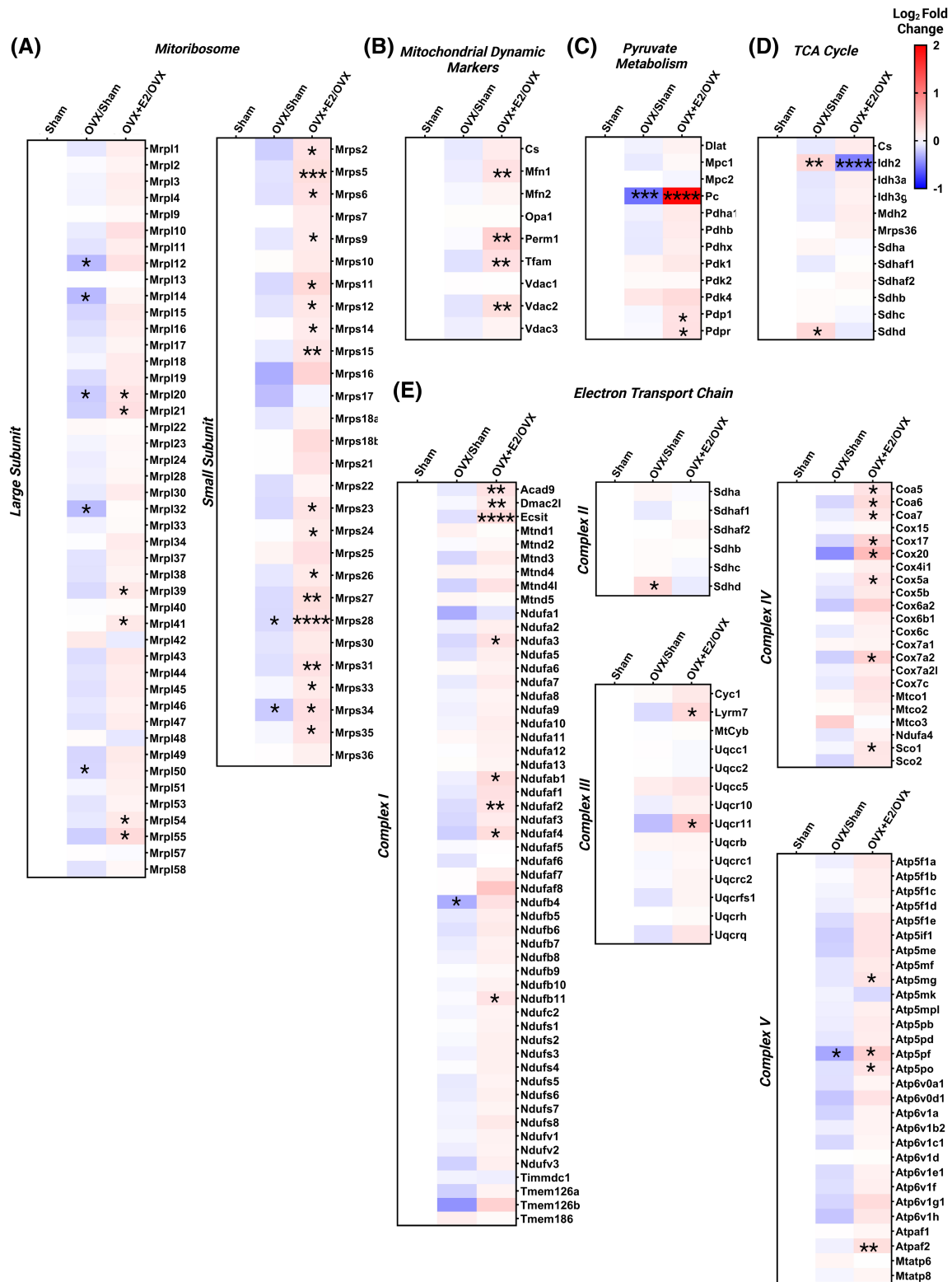


FIGURE 5 Estrogen replacement upregulates proteins associated with mitochondrial dynamics and metabolism in female *mdx* mice. The proteomics dataset was probed for proteins associated with the mitoribosome, mitochondrial dynamics and metabolism and are displayed as heatmaps with ovariectomized (OVX) compared to Sham and OVX + E2 (estradiol) compared to OVX. The impact of OVX, and E2 replacement, is demonstrated on (A) the mitoribosome, (B) markers of mitochondrial dynamics, (C) pyruvate metabolism, (D) the tricarboxylic acid (TCA) cycle and (E) the electron transport chain. * $p < .05$, ** $p < .01$, *** $p < .001$, **** $p < .0001$ OVX versus Sham or OVX + E2 versus OVX. Sham $n = 5$; OVX $n = 6$; OVX + E2 $n = 6$.

There was a very weak association between Rbm20 expression and exercise capacity ($r^2 < .3$; Figure 6A) and each intermediate of the TCA cycle ($r^2 < .3$; Figure 6B–G) but there was moderate association between CS activity and Rbm20 protein levels ($r^2 = .5305$, $p < .01$; Figure 6H). Although a very weak association between Rbm20 and Cs ($p = .0876$; Figure 6I), Mfn2 (Figure 6J), Opa1 (Figure 6K), Vdac1 (Figure 6L), and -3 (Figure 6M; all $r^2 < .3$) protein expression was detected, other markers of mitochondrial content and biogenesis, including Mfn1 ($p < .001$, Figure 6N), Tfam ($p < .001$, Figure 6O), and Vdac2 ($p < .0001$, Figure 6P) had a moderate association with Rbm20 expression while Perml was weakly associated ($r^2 = .4861$, $p < .01$, Figure 6Q). Pc protein expression was most strongly associated with Rbm20 expression ($r^2 = .9398$, $p < .0001$; Figure 6R).

4 | DISCUSSION

Despite expressing dystrophin (albeit to varying degrees^{46,47}), female DMD carriers manifest exercise intolerance and metabolic anomalies, including delayed recovery of high phosphate energy.¹⁸ These are likely to be exacerbated following menopause since estrogen is known to regulate skeletal muscle function and metabolism by positively regulating mitochondrial biogenesis, respiratory chain respiration, and lipid metabolism.⁴⁸ Our study confirms that OVX reduces exercise capacity, serum TCA cycle intermediate concentration, and muscle CS activity in female *mdx* mice. Moreover, replacement of estrogen with E2 offset these deficits, supporting the idea that loss of estrogen could exacerbate dystropathology in female DMD carriers. In OVX mice, proteomics analysis identified a reduction in Rbm20, a critical regulator of sarcomeric and muscle homeostasis gene splicing. This was associated with changes in the skeletal muscle proteome that reflected reduced ribosomal and mitochondrial activity. Estradiol replacement attenuated the downregulation of the Rbm20 protein that was observed in the OVX-only group and promoted metabolic and mitochondrial processes, suggesting that estrogen allays the dystrophic phenotype of female DMD carriers.

Exercise intolerance is a well-documented effect following the loss of estrogen (previously reviewed in^{48,49}) and our findings support this notion since OVX mice had a significantly reduced exercise capacity (~64%), which was normalized by E2 replacement. Since exercise capacity is linked with metabolism, we probed our published serum metabolome dataset²⁶ to elucidate a pathway/s which could, in part, explain the observed deficits in exercise. We determined that TCA cycle intermediates were reduced in OVX mice – specifically succinate and cis-aconitate concentration. In ER-related- α (ERR α) KO mice, muscle TCA

cycle intermediates, including succinate, are reduced following exercise, however, we did not see an accumulation of other intermediates (e.g., citrate or cis-aconitate) as observed in Perry et al.⁵⁰ This could be explained by either the difference in intensity of the exercise tests employed or the fact that our study used OVX to reduce estrogen levels while Perry et al. utilized ERR α KO to reduce estrogen binding to skeletal muscle while maintaining circulating levels. We did not quantify whether OVX completely abolished circulating estrogen (confirmed with reductions in uterus mass), thus our findings may be reflective of residual circulating estrogen, which has been previously demonstrated in rats one-month post OVX.⁵¹ Irrespective, our data indicate that loss of estrogen production via OVX impacts TCA cycle flux. For succinate, the reduced concentration appears reflective of increased succinate oxidation (SDH capacity significantly increased in the TA and trend in the diaphragm). In particular, the Sdh subunit of CII, which is responsible for terminal electron transfer flow to CoQ and coordinating succinate oxidation, was specifically upregulated by OVX whereas Sdhb subunit, a traditional biomarker of Complex II content, was not. Increasing SDH/CII flux may be a compensatory mechanism in response to OVX as loss of estrogen has been shown to decrease CI respiration in skeletal muscle.⁵² However, this finding contradicts other studies which demonstrate reduced SDH following ovariectomy or ERR KO.^{53–55} Most likely, our conflicting data are related to either the protocol employed to prevent estrogens' effect on skeletal muscle (i.e., reduced estrogen levels versus KO of the receptor) or the length of time between OVX and testing as estrogen levels can fluctuate due to extragonadal aromatization of estrogen.⁵¹

Given that OVX altered the concentration of TCA cycle intermediates, we anticipated that proteins associated with metabolism would be impacted by OVX in skeletal muscle. To the contrary, only Rbm20 met the statistically significant criteria (0.75 log₂ fold change, adjusted $p < .05$), which was downregulated following OVX. To the best of our knowledge, this is the first time that OVX has been shown to impact Rbm20 expression. Rbm20 is a post-transcriptional splicer abundant in both skeletal and cardiac muscle and known to have more than 30 splicing targets (for a comprehensive review, see⁴⁵). These targets have functions in various pathways, including cytoskeleton organisation,^{56,57} contraction,⁵⁶ and calcium handling,^{56,57} all of which are affected in DMD.^{58,59} More recently, loss of Rbm20 has been linked to impaired mitochondrial function and dysregulated metabolic pathways and processes. In Rbm20 KO rats, mitochondrial respiration, particularly driven by CI, is reduced⁶⁰ and metabolic pathways are downregulated,⁶¹ indicating that Rbm20 is an essential regulator of metabolism. While our pathways

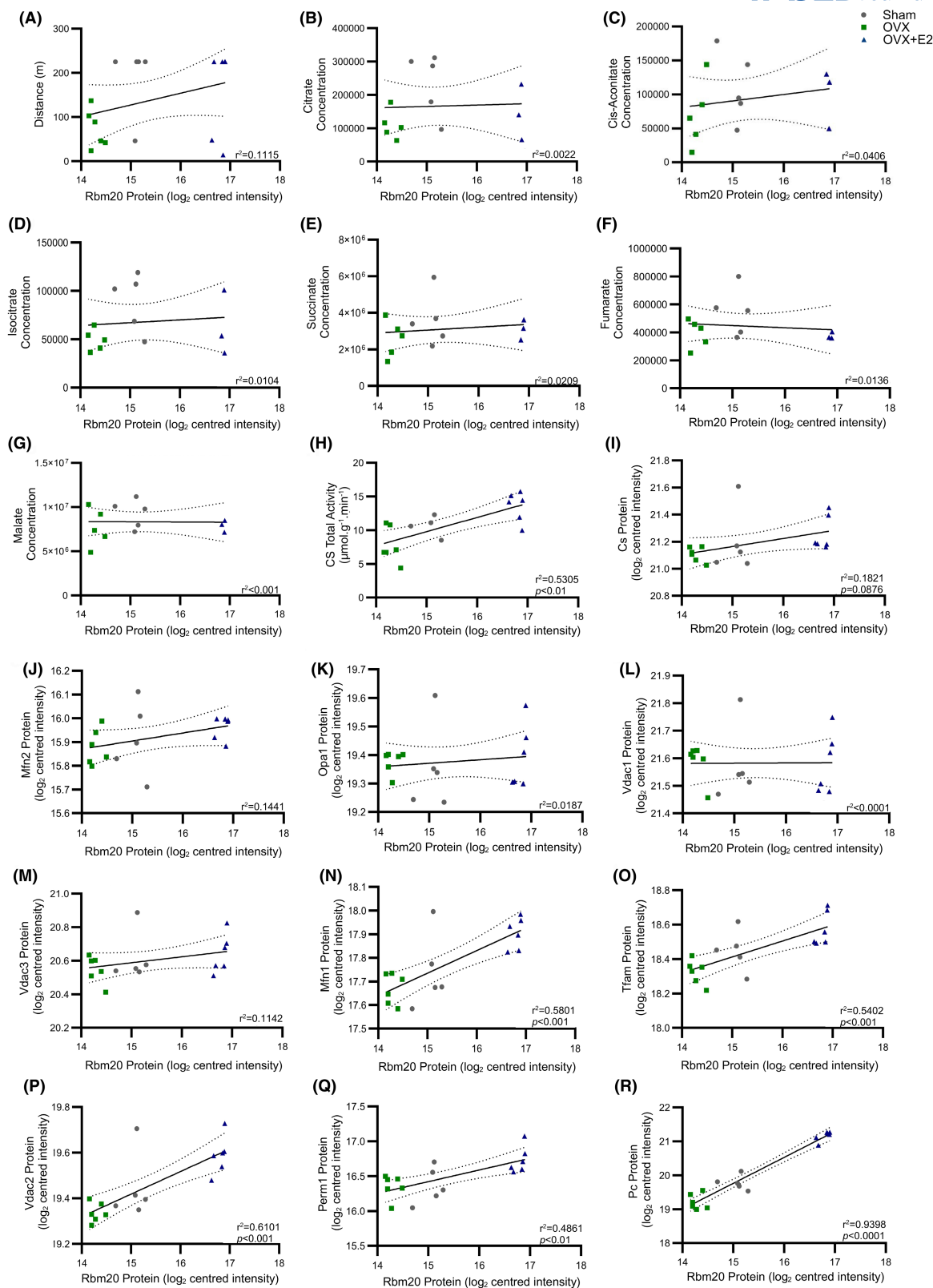


FIGURE 6 Rbm20 protein expression is associated with key metabolic indices in female *mdx* mice. Rbm20 protein expression of skeletal muscle was correlated with exercise capacity (A), the tricarboxylic acid cycle intermediates (B–G), citrate synthase (CS) activity (H), markers of mitochondrial dynamics (I–Q) and pyruvate carboxylase (Pc) protein expression (R) in Sham, ovariectomized (OVX), and OVX with estradiol (E2) replacement (OVX + E2) mice. The coefficient of determination (r^2) is noted in each panel with the dotted lines denoting the 95% confidence intervals. Sham $n=4-5$; OVX $n=5-6$; OVX + E2 $n=3-6$.

analysis of the proteome did not indicate up- or downregulation of metabolic pathways (OVX vs Sham), E2 replacement did modulate many metabolic and mitochondrial processes, including the control of mitochondrial calcium uptake proteins, which were associated with upregulation of Rbm20, strengthening the idea that Rbm20 protein expression is responsive to fluctuations in estrogen. Although speculative, the mechanism may be coordinated through ER α which (1) is a known modulator of metabolism,⁶² (2) is responsive to other clock-related genes⁶³ and (3) regulates the estrogen response element (ERE) on some circadian rhythm genes.^{64,65} Confirming whether Rbm20 is directly modulated by ER binding is an important next step in understanding the influence of hormones and the circadian clock on the regulation of muscle metabolism and function.

E2 replacement upregulated various metabolic and mitochondrial pathways suggesting proteins associated with mitochondrial dynamics, the TCA cycle and the ETC could be affected. While most of the proteins investigated were not statistically different following OVX (compared to Sham), our metabolomics data suggested changes in mitochondrial dynamics and/or TCA function, indicating biologically relevant (albeit non-statistically significant) changes to the mitochondrial proteome. The loss of estrogen/OVX or ER α KO downregulates metabolism^{50,53–55,66} and our data infer early adaptations at 4–5 weeks post-OVX. Increasing the duration of estrogen deprivation would likely lead to widespread reductions in the expression of mitochondrial and metabolic proteins. A similar scenario is observed with E2 replacement, with our analysis suggesting an overall upregulation of mitochondrial dynamic markers and metabolic proteins. For example, upregulation of Mfn1 is associated with improved bioenergetics, calcium handling, and excitation-contraction coupling in muscle.⁶⁷ Corresponding upregulation of the master mitochondrial DNA transcription factor, Tfam, and transcription of oxidative metabolic machinery (e.g., Ndufa2, Uqcrl1, Cox20, Atpaf2) to facilitate bioenergetic adaptations were observed. Others have also demonstrated that E2 replacement via implant, as used in this study, increases mitochondrial enzyme activity.^{68,69} When considered in conjunction with our data, this suggests that estrogen controls both enzyme expression and kinetics via orchestrating substrate flux. It is important to note however, that implantable hormone systems deliver sustained E2 concentrations in comparison to the cyclical circadian release that is observed in vivo,⁶⁶ which could lead to supraphysiological levels⁶⁸ and evoke an exaggerated mitochondrial/metabolic response.

Pc was the second most upregulated protein following E2 replacement indicating this could be a primary

mechanism of estrogen's effect on metabolism. OVX downregulated Pc (\log_2 fold change = -0.561 , $p < .001$) but had no impact on any of the other proteins associated with pyruvate metabolism. Pc is responsible for the conversion of pyruvate to oxaloacetate, a TCA cycle intermediate, and its anaplerotic action is critical for pacing TCA cycle flux while fostering biosynthesis pathways (e.g., gluconeogenesis and lipogenesis⁷⁰). Pc KO mice have impaired TCA cycle metabolism, resulting in a $\sim 50\%$ reduction in TCA cycle intermediates.⁷¹ While pyruvate can also be metabolized by a second enzyme, pyruvate dehydrogenase (PDH), which converts pyruvate into acetyl CoA to drive the TCA cycle, we did not observe any differences in the PDH subunits following OVX nor the pyruvate transporters (Mpc1 and Mpc2). Our data support previous findings indicating that OVX-induced reductions in substrate metabolism are not due to changes in the protein expression of PDH, Mpc1 or Mpc2.⁶⁶ Instead, our data suggest that the downregulation of Pc may be partially responsible for the reduction in TCA cycle intermediates, particularly since E2 replacement upregulated Pc expression and normalized serum TCA cycle intermediates. Indeed, compensatory upregulation of Pc protein (and activity) anaplerotically rescues TCA cycle intermediate perturbations in cardiomyocyte-deficient C2C12 muscle cells,⁷² indicating a critical role of Pc in maintaining TCA flux. Serum metabolite concentrations are a good reflection of lean tissue metabolite levels⁴³ because TCA cycle intermediates – particularly succinate – act as metabolites to signal and modulate systemic energy metabolism.⁷³

Dilated cardiomyopathy is a common complication of female DMD carriers^{74–78} that is often attributed to the mosaic dystrophin expression observed in cardiac tissue.^{74,75,79} Our data indicate that reduced Rbm20 may also contribute to this morbidity, particularly in peri-/menopausal female carriers given OVX downregulated Rbm20 expression. Loss of function mutation of Rbm20 causes dilated cardiomyopathy (both of genetic and non-genetic origins⁴⁵). Rbm20 KO rodents and human iPSC-derived Rbm20 mutant cardiomyocytes show impaired cardiac contractility and myocardial stiffness, which is attributed to mis-splicing of calcium-handling genes, for example, *Ryr2* and *Camk2a*,^{80,81} as well as impaired Frank–Starling mechanism due to mis-splicing of *TTN* (titin^{56,82}). These same pathophysiological features were recently documented in human iPSC-derived cardiomyocytes from a female Becker MD carrier engineered to have a DMD mutation.⁸³ While neither Rbm20 expression, nor its splicing targets, were investigated in the study by Kameda et al., the similarities in cardiac abnormalities between Rbm20-induced dilated cardiomyopathy and cardiomyopathy in female DMD carriers are evident and suggest that further

research is warranted to ascertain the role of Rbm20 in female DMD carrier cardiomyopathy.

Research on Rbm20 in the context of skeletal muscle is limited. However, evidence suggests that it controls sarcomere assembly and passive elasticity. Loss of Rbm20 shifts Ttn from the stiff to the compliant isoform,^{84,85} a phenotype that reduces contractility manifesting as muscle weakness and exercise intolerance.⁸⁶ While Ttn isoforms (and levels) have yet to be quantitated in female DMD carriers, muscle weakness and exercise intolerance are common physiological symptoms^{87,88} – further research is warranted to confirm whether Ttn, and indeed Rbm20, are mediators. No effect of OVX or E2 replacement on Ttn protein expression (\log_2 fold = 0.0112, $p = .901$ and \log_2 fold = -0.0847, $p = .332$, respectively) was observed, but this does not rule out a potential shift in Ttn isoforms. Thyroid hormone was shown to regulate titin isoform transition via Rbm20 in cardiomyocytes,⁸⁹ suggesting other hormones, for example, E2, may also be influential. Furthermore, loss of Rbm20 in skeletal muscle diminishes exercise capacity,⁹⁰ which may partly explain the decreased exercise capacity observed in OVX mice.

Recently, Rbm20 was shown to regulate Ttn splicing in skeletal muscle under the control of the muscle circadian clock regulatory genes, *Bmal1* and *Clock*.³² There is well-established reciprocal regulation between circadian and estrogen signaling (for a review, see Alvord et al.⁶³). The suprachiasmatic nucleus (SCN) is the master timekeeper of the circadian rhythm, and although there is no evidence that it is directly modulated by circulating estrogen rhythms, our pathways analysis suggests OVX might alter SCN-mediated timekeeping via changes to retinal function or vice versa. Four vision-related pathways involving a total of 26 modulated proteins were upregulated including retinoid metabolism and transport, visual phototransduction, diseases associated with visual transduction, and canonical retinoid cycle in rods (twilight vision). The SCN receives light input from the retina, and via a complex hormonal and neural milieu, orchestrates tissue-specific transcription of Cryptochrome (*Cry*) 1 and 2 and Period (*Per*) 1, 2 and 3 genes by *Bmal1* and *Clock*, to induce local circadian effects.⁶⁴ ER α and - β are outputs of the molecular clock transcription program but can also directly regulate the estrogen response element (ERE) on specific circadian genes such as *Per2*^{64,91,92} and *Clock*.^{65,93} ER α expression (\log_2 fold = -0.532, $p = .13$) was not significantly affected by OVX in our muscle proteome but E2 replacement did upregulate expression (\log_2 fold = 0.861, $p = .0155$; ER β was not detected). In rodent metabolic tissues, OVX results in a significant circadian phase shift of *Per1* expression (liver) and/or a rapid decline in circadian phase synchrony (liver and white adipose tissue) with impact on lipid metabolism, insulin sensitivity and glucose tolerance

in these tissues. Our data suggest a nexus exists between estrogen, Rbm20 expression, and the regulation of metabolism. Rbm20 was strongly correlated with *Pc* expression. However, whether they are mutually but independently regulated by circulating estrogen levels, or whether, the expression of one protein, for example, *Pc* is dependent on the other, for example, Rbm20 is unknown. Since Rbm20 function was recently linked to circadian clock control of skeletal muscle, this may be the one fundamental mechanism controlling the entire nexus and downstream effects on muscle metabolism and function. However, detailed studies will be required to decipher these intricacies.

5 | CONCLUSION

To our knowledge, this is the first study to link the loss of estrogen and changes to muscle metabolism with Rbm20 protein expression. Our data indicate estrogen may play a role in reducing the dystrophinopathic characteristics in female *mdx* mice and protects against exercise intolerance. Importantly, OVX downregulated Rbm20 protein expression, which may contribute to common female DMD carrier manifestations (e.g., dilated cardiomyopathy and exercise intolerance). Further research is required to confirm whether the decrease in Rbm20 protein is also associated with a reduction in Rbm20 splicing capacity.

While the use of tamoxifen, a selective ER α agonist, does not appear to be clinically beneficial for DMD patients,³⁰ our data indicate that E2 replacement could be valuable for female DMD carriers (above menopausal age). A notable limitation of our study is that we used homozygous females with complete dystrophin deficiency (aside from spontaneous revertant fibers characteristic of the *mdx* model), whereas female DMD carriers are typically heterozygous for the *DMD* mutation. There may be notable muscular system differences in response to estrogen depletion and repletion due to genotype or species, which lessen the translational aspect of our study. Studying the impact of ovariectomy on Rbm20 expression in other mouse models that better mimic the genotype and phenotype of female DMD carriers, for example, the heterozygous female *mdx* mouse which display metabolic abnormalities,¹³ or the *mdx-Xist^{Ahs}* female mouse which expresses mosaic but persistently low dystrophin levels and functional deficits,⁹⁴ could shed more light. Dystrophic-like features in female carriers can manifest from as young as 3 years of age,⁹⁵ which indicates that E2 therapy may not be a universal treatment option for carriers. The inclusion of a Sham+E2 repletion group would have been beneficial to identify any possible off-target effect of supraphysiological E2 in this regard. Follow-up studies are warranted to understand whether estrogen levels correlate with severity/onset of

dystrophinopathy in female carriers and if E2 replacement is a viable therapeutic pathway.

AUTHOR CONTRIBUTIONS

A. Lindsay and E. Rybalka conceived and designed the research; C.A. Timpani, D. Debrincat, S. Kourakis, R. Boyer, L.E. Formosa, J.R. Steele, H. Zhang, R.B. Schittenhelm, E. Rybalka, and A. Lindsay conducted the experiments and interpreted the results; C.A. Timpani and E. Rybalka prepared the manuscript, and all authors were involved in critically reviewing the manuscript.

ACKNOWLEDGMENTS

This research was supported by a Deakin University HAAtCH Grant (awarded to A.L.) and an Institute for Physical Activity and Nutrition Seed Grant (awarded to A.L.). A.L. was supported by a Philip Wrightson Fellowship (Neurological Foundation) and is currently supported by a Sir Charles Hercus Health Research Fellowship (Health Research Council). L.E.F. is supported by a National Health and Medical Research Council (NHMRC) Investigator Grant (GNT2010149) and funding from the Mito Foundation. C.A.T and E.R. are supported by AFM Téléthon (France). Open access publishing facilitated by University of Canterbury, as part of the Wiley - University of Canterbury agreement via the Council of Australian University Librarians.

DISCLOSURES

The authors declare no conflicts of interest.

DATA AVAILABILITY STATEMENT

Data will be made available upon reasonable request from the corresponding author.

ORCID

Cara A. Timpani  <https://orcid.org/0000-0003-4567-4319>

Didier Debrincat  <https://orcid.org/0009-0007-7610-8471>

Stephanie Kourakis  <https://orcid.org/0000-0001-5683-9989>

Luke E. Formosa  <https://orcid.org/0000-0002-7740-6151>

Joel R. Steele  <https://orcid.org/0000-0002-3070-9761>

Haijian Zhang  <https://orcid.org/0009-0004-8479-8132>

Ralf B. Schittenhelm  <https://orcid.org/0000-0001-8738-1878>

Aaron P. Russell  <https://orcid.org/0000-0002-7323-9501>

Emma Rybalka  <https://orcid.org/0000-0002-4854-0036>

Angus Lindsay  <https://orcid.org/0000-0002-5195-1901>

REFERENCES

1. Timpani CA, Hayes A, Rybalka E. Revisiting the dystrophin-ATP connection: how half a century of research still implicates mitochondrial dysfunction in Duchenne muscular dystrophy aetiology. *Med Hypotheses*. 2015;85:1021-1033.
2. Budzinska M, Zimna A, Kurpisz M. The role of mitochondria in Duchenne muscular dystrophy. *J Physiol Pharmacol*. 2021;72:157-166. doi:10.26402/jpp.2021.2.01
3. Lindsay A, Chamberlain CM, Witthuhn BA, Lowe DA, Ervasti JM. Dystrophinopathy-associated dysfunction of Krebs cycle metabolism. *Hum Mol Genet*. 2018;28:942-951. doi:10.1093/hmg/ddy404
4. Tsonaka R, Signorelli M, Sabir E, et al. Longitudinal metabolomic analysis of plasma enables modeling disease progression in Duchenne muscular dystrophy mouse models. *Hum Mol Genet*. 2020;29:745-755. doi:10.1093/hmg/ddz309
5. Dabaj I, Ferey J, Marguet F, et al. Muscle metabolic remodeling patterns in Duchenne muscular dystrophy revealed by ultra-high-resolution mass spectrometry imaging. *Sci Rep*. 2021;11:1906. doi:10.1038/s41598-021-81090-1
6. Ramos SV, Hughes MC, Delfinis LJ, Bellissimo CA, Perry CGR. Mitochondrial bioenergetic dysfunction in the D2.mdx model of Duchenne muscular dystrophy is associated with microtubule disorganization in skeletal muscle. *PLoS One*. 2020;15:e0237138. doi:10.1371/journal.pone.0237138
7. Timpani CA, Trewin AJ, Stojanovska V, et al. Attempting to compensate for reduced neuronal nitric oxide synthase protein with nitrate supplementation cannot overcome metabolic dysfunction but rather has detrimental effects in dystrophin-deficient mdx muscle. *Neurotherapeutics*. 2017;14:429-446.
8. Mareedu S, Million ED, Duan D, Babu GJ. Abnormal calcium handling in Duchenne muscular dystrophy: mechanisms and potential therapies. *Front Physiol*. 2021;12:647010. doi:10.3389/fphys.2021.647010
9. Rybalka E, Timpani CA, Stathis CG, Hayes A, Cooke MB. Metabogenic and nutraceutical approaches to address energy dysregulation and skeletal muscle wasting in duchenne muscular dystrophy. *Nutrients*. 2015;7:9734-9767.
10. Vu Hong A, Sanson M, Richard I, Israeli D. A revised model for mitochondrial dysfunction in Duchenne muscular dystrophy. *European Journal of Translational Myology*. 2021;31:10012. doi:10.4081/ejtm.2021.10012
11. Luan P, D'Amico D, Andreux PA, et al. Urolithin a improves muscle function by inducing mitophagy in muscular dystrophy. *Sci Transl Med*. 2021;13:eabb0319. doi:10.1126/scitranslmed.abb0319
12. Onopiuk M, Brutkowski W, Wierzbicka K, et al. Mutation in dystrophin-encoding gene affects energy metabolism in mouse myoblasts. *Biochem Biophys Res Commun*. 2009;386:463-466.
13. Moore TM, Lin AJ, Strumwasser AR, et al. Mitochondrial dysfunction is an early consequence of partial or complete dystrophin loss in mdx mice. *Front Physiol*. 2020;11:690. doi:10.3389/fphys.2020.00690
14. Mohiuddin M, Choi JJ, Lee NH, et al. Transplantation of muscle stem cell mitochondria rejuvenates the bioenergetic function of dystrophic muscle. *bioRxiv*. 2020.2004.2017.017822 2020. doi:10.1101/2020.04.17.017822
15. Licandro SA, Crippa L, Pomarico R, et al. The pan HDAC inhibitor Givinostat improves muscle function and histological

- parameters in two Duchenne muscular dystrophy murine models expressing different haplotypes of the LTBP4 gene. *Skelet Muscle*. 2021;11:19. doi:10.1186/s13395-021-00273-6
16. Timpani CA, Kourakis S, Debruin DA, et al. Dimethyl fumarate modulates the dystrophic disease program following short-term treatment. *JCI Insight*. 2023;8:e165974. doi:10.1172/jci.insight.165974
 17. Lee T, Takeshima Y, Kusunoki N, et al. Differences in carrier frequency between mothers of Duchenne and Becker muscular dystrophy patients. *J Hum Genet*. 2014;59:46-50. doi:10.1038/jhg.2013.119
 18. Barbiroli B, Funicello R, Ferlini A, Montagna P, Zaniol P. Muscle energy metabolism in female DMD/BMD carriers: a 31P-MR spectroscopy study. *Muscle Nerve*. 1992;15:344-348. doi:10.1002/mus.880150313
 19. Barbiroli B, McCully KK, Iotti S, Lodi R, Zaniol P, Chance B. Further impairment of muscle phosphate kinetics by lengthening exercise in DMD/BMD carriers: an in vivo 31P-NMR spectroscopy study. *J Neurol Sci*. 1993;119:65-73. doi:10.1016/0022-510X(93)90192-2
 20. Gaines RF, Puschel SM, Sassaman EA, Driscoll JL. Effect of exercise on serum creatine kinase in carriers of Duchenne muscular dystrophy. *J Med Genet*. 1982;19:4-7. doi:10.1136/jmg.19.1.4
 21. Giliberto F, Radic CP, Luce L, Ferreiro V, de Brasi C, Szijan I. Symptomatic female carriers of Duchenne muscular dystrophy (DMD): genetic and clinical characterization. *J Neurol Sci*. 2014;336:36-41. doi:10.1016/j.jns.2013.09.036
 22. Song TJ, Lee KA, Kang SW, Cho H, Choi YC. Three cases of manifesting female carriers in patients with Duchenne muscular dystrophy. *Yonsei Med J*. 2011;52:192-195. doi:10.3349/ymj.2011.52.1.192
 23. Quak ZX, Tan SML, Tan KB, Lin W, Chai P, Ng KWP. A manifesting female carrier of Duchenne muscular dystrophy: importance of genetics for the dystrophinopathies. *Singapore Med J*. 2023;64:81-87. doi:10.4103/singaporemedj.SMJ-2021-356
 24. Ohtani H, Saotome M, Sakamoto A, Suwa K, Maekawa Y. Drug-refractory heart failure in female carrier of Duchenne muscular dystrophy: a case of X-linked dilated cardiomyopathy. *Intern Med*. 2023;62:2089-2092. doi:10.2169/internalmedicine.0745-22
 25. Lindsay A, Russell AP. The unconditioned fear response in dystrophin-deficient mice is associated with adrenal and vascular function. *Sci Rep*. 2023;13:5513.
 26. Lindsay A, Trewin AJ, Sadler KJ, Laird C, Della Gatta PA, Russell AP. Sensitivity to behavioral stress impacts disease pathogenesis in dystrophin-deficient mice. *FASEB J*. 2021;35:e22034.
 27. Lowe DA, Kararigas G. Editorial: new insights into estrogen/estrogen receptor effects in the cardiac and skeletal muscle. *Front Endocrinol*. 2020;11:141. doi:10.3389/fendo.2020.00141
 28. Dorchie OM, Reutenauer-Patte J, Dahmane E, et al. The anticancer drug tamoxifen counteracts the pathology in a mouse model of Duchenne muscular dystrophy. *Am J Pathol*. 2013;182:485-504. doi:10.1016/j.ajpath.2012.10.018
 29. Birnbaum F, Eguchi A, Pardon G, Chang ACY, Blau HM. Tamoxifen treatment ameliorates contractile dysfunction of Duchenne muscular dystrophy stem cell-derived cardiomyocytes on bioengineered substrates. *Npj Regen Med*. 2022;7:19. doi:10.1038/s41536-022-00214-x
 30. Henzi BC, Schmidt S, Nagy S, et al. Safety and efficacy of tamoxifen in boys with Duchenne muscular dystrophy (TAMDMD): a multicentre, randomised, double-blind, placebo-controlled, phase 3 trial. *Lancet Neurol*. 2023;22:890-899. doi:10.1016/S1474-4422(23)00285-5
 31. Nagy S, Hafner P, Schmidt S, et al. Tamoxifen in Duchenne muscular dystrophy (TAMDMD): study protocol for a multicenter, randomized, placebo-controlled, double-blind phase 3 trial. *Trials*. 2019;20:637. doi:10.1186/s13063-019-3740-6
 32. Riley LA, Zhang X, Douglas CM, et al. The skeletal muscle circadian clock regulates titin splicing through RBM20. *eLife*. 2022;11:e76478. doi:10.7554/eLife.76478
 33. Prisby RD, Dominguez JM II, Muller-Delp J, Allen MR, Delp MD. Aging and estrogen status: a possible endothelium-dependent vascular coupling mechanism in bone remodeling. *PLoS One*. 2012;7:e48564. doi:10.1371/journal.pone.0048564
 34. Mann SN, Pitel KS, Nelson-Holte MH, et al. 17 α -estradiol prevents ovariectomy-mediated obesity and bone loss. *Exp Gerontol*. 2020;142:111113. doi:10.1016/j.exger.2020.111113
 35. Timpani CA, Goodman CA, Stathis CG, et al. Adenylosuccinic acid therapy ameliorates murine Duchenne muscular dystrophy. *Sci Rep*. 2020;10:1125. doi:10.1038/s41598-020-57610-w
 36. Rybalka E, Timpani CA, Cooke MB, Williams AD, Hayes A. Defects in mitochondrial ATP synthesis in dystrophin-deficient mdx skeletal muscles may be caused by complex I insufficiency. *PLoS One*. 2014;9:e115763.
 37. HaileMariam M, Eguez RV, Singh H, et al. S-trap, an ultrafast sample-preparation approach for shotgun proteomics. *J Proteome Res*. 2018;17:2917-2924. doi:10.1021/acs.jproteome.8b00505
 38. Shah AD, Goode RJA, Huang C, Powell DR, Schittenhelm RB. LFQ-analyst: an easy-to-use interactive web platform to analyze and visualize label-free proteomics data preprocessed with MaxQuant. *J Proteome Res*. 2020;19:204-211. doi:10.1021/acs.jproteome.9b00496
 39. Zhang H, Steele JR, Kahrood HV, Lucas DD, Shah AD, Schittenhelm RB. Phospho-analyst: an interactive, easy-to-use web platform to analyze quantitative Phosphoproteomics data. *J Proteome Res*. 2023;22:2890-2899. doi:10.1021/acs.jproteome.3c00186
 40. Zhang X, Smits AH, van Tilburg GBA, Ovaas H, Huber W, Vermeulen M. Proteome-wide identification of ubiquitin interactions using UbIA-MS. *Nat Protoc*. 2018;13:530-550. doi:10.1038/nprot.2017.147
 41. Ritchie ME, Phipson B, Wu D, et al. Limma powers differential expression analyses for RNA-sequencing and microarray studies. *Nucleic Acids Res*. 2015;43:e47. doi:10.1093/nar/gkv007
 42. Gillespie M, Jassal B, Stephan R, et al. The reactome pathway knowledgebase 2022. *Nucleic Acids Res*. 2021;50:D687-D692. doi:10.1093/nar/gkab1028
 43. Dutta T, Chai HS, Ward LE, et al. Concordance of changes in metabolic pathways based on plasma metabolomics and skeletal muscle Transcriptomics in type 1 diabetes. *Diabetes*. 2012;61:1004-1016. doi:10.2337/db11-0874
 44. O'Leary MF, Jackman SR, Bowtell JL. Shatavari supplementation in postmenopausal women alters the skeletal muscle proteome and pathways involved in training adaptation. *Eur J Nutr*. 2024;63:869-879. doi:10.1007/s00394-023-03310-w
 45. Koelemen J, Gotthardt M, Steinmetz LM, Meder B. RBM20-related cardiomyopathy: current understanding and future options. *J Clin Med*. 2021;10:4101. doi:10.3390/jcm10184101

46. Cotta A, Paim JF, Carvalho E, et al. Phenotypic variability of Dystrophinopathy symptomatic female carriers. *Can J Neurol Sci.* 2017;44:304-310. doi:10.1017/cjn.2016.448
47. Romero NB, de Lonlay P, Lléns S, et al. Pseudo-metabolic presentation in a Duchenne muscular dystrophy symptomatic carrier with 'de novo' duplication of dystrophin gene. *Neuromuscul Disord.* 2001;11:494-498. doi:10.1016/S0960-8966(01)00192-4
48. Ikeda K, Horie-Inoue K, Inoue S. Functions of estrogen and estrogen receptor signaling on skeletal muscle. *J Steroid Biochem Mol Biol.* 2019;191:105375. doi:10.1016/j.jsbmb.2019.105375
49. Pellegrino A, Tiidus PM, Vandenboom R. Mechanisms of estrogen influence on skeletal muscle: mass, regeneration, and mitochondrial function. *Sports Med.* 2022;52:2853-2869. doi:10.1007/s40279-022-01733-9
50. Perry MC, Dufour CR, Tam IS, B'Chir W, Giguère V. Estrogen-related receptor- α coordinates transcriptional programs essential for exercise tolerance and muscle fitness. *Mol Endocrinol.* 2014;28:2060-2071. doi:10.1210/me.2014-1281
51. Zhao H, Tian Z, Hao J, Chen B. Extragonadal aromatization increases with time after ovariectomy in rats. *Reprod Biol Endocrinol.* 2005;3:6. doi:10.1186/1477-7827-3-6
52. Torres MJ, Ryan TE, Lin CT, Zeczycki TN, Neuffer PD. Impact of 17 β -estradiol on complex I kinetics and H₂O₂ production in liver and skeletal muscle mitochondria. *J Biol Chem.* 2018;293:16889-16898. doi:10.1074/jbc.RA118.005148
53. Siebert C, Kolling J, Scherer EBS, et al. Effect of physical exercise on changes in activities of creatine kinase, cytochrome c oxidase and ATP levels caused by ovariectomy. *Metab Brain Dis.* 2014;29:825-835. doi:10.1007/s11011-014-9564-x
54. Watzet J-S, Eury E, Hazen BC, et al. Loss of skeletal muscle estrogen-related receptors leads to severe exercise intolerance. *Molecular Metabolism.* 2023;68:101670. doi:10.1016/j.molmet.2023.101670
55. Torres MJ, Kew KA, Ryan TE, et al. 17 β -estradiol directly lowers mitochondrial membrane microviscosity and improves bioenergetic function in skeletal muscle. *Cell Metab.* 2018;27:167-179.e167. doi:10.1016/j.cmet.2017.10.003
56. Guo W, Schafer S, Greaser ML, et al. RBM20, a gene for hereditary cardiomyopathy, regulates titin splicing. *Nat Med.* 2012;18:766-773. doi:10.1038/nm.2693
57. Maatz H, Jens M, Liss M, et al. RNA-binding protein RBM20 represses splicing to orchestrate cardiac pre-mRNA processing. *J Clin Invest.* 2014;124:3419-3430. doi:10.1172/JCI74523
58. Rybalka E, Timpani C, Debruin D, Bagaric R, Campelj D, Hayes A. The failed clinical story of myostatin inhibitors against Duchenne muscular dystrophy: exploring the biology behind the battle. *Cells.* 2020;9:2657. doi:10.3390/cells9122657
59. Kourakis S, Timpani CA, de Haan JB, Gueven N, Fischer D, Rybalka E. Targeting Nrf2 for the treatment of Duchenne muscular dystrophy. *Redox Biol.* 2021;38:101803. doi:10.1016/j.redox.2020.101803
60. Vad OB, Angeli E, Liss M, et al. Loss of cardiac splicing regulator RBM20 is associated with early-onset atrial fibrillation. *JACC: Basic to Translational Science.* 2024;9:163-180. doi:10.1016/j.jacbts.2023.08.008
61. Larson EJ, Gregorich ZR, Zhang Y, et al. Rbm20 ablation is associated with changes in the expression of titin-interacting and metabolic proteins. *Molecular Omics.* 2022;18:627-634. doi:10.1039/D2MO00115B
62. Hevener AL, Ribas V, Moore TM, Zhou Z. The impact of skeletal muscle ER α on mitochondrial function and metabolic health. *Endocrinology.* 2020;161:bqz017. doi:10.1210/endo/bqz017
63. Alvord VM, Kantra EJ, Pendergast JS. Estrogens and the circadian system. *Semin Cell Dev Biol.* 2022;126:56-65. doi:10.1016/j.semcdb.2021.04.010
64. Nakamura TJ, Moriya T, Inoue S, et al. Estrogen differentially regulates expression of Per1 and Per2 genes between central and peripheral clocks and between reproductive and nonreproductive tissues in female rats. *J Neurosci Res.* 2005;82:622-630. doi:10.1002/jnr.20677
65. Xiao L, Chang AK, Zang MX, et al. Induction of the CLOCK gene by E2-ER α signaling promotes the proliferation of breast cancer cells. *PLoS One.* 2014;9:e95878. doi:10.1371/journal.pone.0095878
66. Takahashi K, Kitaoka YU, Matsunaga Y, Hatta H. Effects of endurance training on metabolic enzyme activity and transporter proteins in skeletal muscle of Ovariectomized mice. *Med Sci Sports Exerc.* 2023;55:186-198. doi:10.1249/mss.0000000000003045
67. Eisner V, Lenaers G, Hajnóczky G. Mitochondrial fusion is frequent in skeletal muscle and supports excitation-contraction coupling. *J Cell Biol.* 2014;205:179-195. doi:10.1083/jcb.201312066
68. Campbell SE, Febbraio MA. Effect of ovarian hormones on mitochondrial enzyme activity in the fat oxidation pathway of skeletal muscle. *Am J Physiol Endocrinol Metab.* 2001;281:E803-E808. doi:10.1152/ajpendo.2001.281.4.E803
69. Beckett T, Tchernof A, Toth MJ. Effect of ovariectomy and estradiol replacement on skeletal muscle enzyme activity in female rats. *Metabolism.* 2002;51:1397-1401. doi:10.1053/meta.2002.35592
70. Jitrapakdee S, St Maurice M, Rayment I, Cleland WW, Wallace JC, Attwood PV. Structure, mechanism and regulation of pyruvate carboxylase. *Biochem J.* 2008;413:369-387. doi:10.1042/bj20080709
71. Cappel DA, Deja S, Duarte JAG, et al. Pyruvate-carboxylase-mediated Anaplerosis promotes antioxidant capacity by sustaining TCA cycle and redox metabolism in liver. *Cell Metab.* 2019;29:1291-1305.e1298. doi:10.1016/j.cmet.2019.03.014
72. Li Y, Lou W, Raja V, et al. Cardiolipin-induced activation of pyruvate dehydrogenase links mitochondrial lipid biosynthesis to TCA cycle function. *J Biol Chem.* 2019;294:11568-11578. doi:10.1074/jbc.RA119.009037
73. MacCannell ADV, Roberts LD. Metabokines in the regulation of systemic energy metabolism. *Curr Opin Pharmacol.* 2022;67:102286. doi:10.1016/j.coph.2022.102286
74. Adachi K, Hashiguchi S, Saito M, et al. Detection and management of cardiomyopathy in female dystrophinopathy carriers. *J Neurol Sci.* 2018;386:74-80. doi:10.1016/j.jns.2017.12.024
75. Politano L, Nigro V, Nigro G, et al. Development of cardiomyopathy in female carriers of Duchenne and Becker muscular dystrophies. *JAMA.* 1996;275:1335-1338. doi:10.1001/jama.1996.03530410049032
76. Hoogerwaard EM, Bakker E, Ippel PF, et al. Signs and symptoms of Duchenne muscular dystrophy and Becker muscular dystrophy among carriers in The Netherlands: a cohort study. *Lancet.* 1999;353:2116-2119. doi:10.1016/s0140-6736(98)10028-4

77. Grain L, Cortina-Borja M, Forfar C, Hilton-Jones D, Hopkin J, Burch M. Cardiac abnormalities and skeletal muscle weakness in carriers of Duchenne and Becker muscular dystrophies and controls. *Neuromuscul Disord.* 2001;11:186-191. doi:[10.1016/S0960-8966\(00\)00185-1](https://doi.org/10.1016/S0960-8966(00)00185-1)
78. Schelhorn J, Schoenecker A, Neudorf U, et al. Cardiac pathologies in female carriers of Duchenne muscular dystrophy assessed by cardiovascular magnetic resonance imaging. *Eur Radiol.* 2015;25:3066-3072. doi:[10.1007/s00330-015-3694-3](https://doi.org/10.1007/s00330-015-3694-3)
79. Florian A, Ludwig A, Ong P, et al. Cause of cardiac disease in a female carrier of Duchenne muscular dystrophy. *Circulation.* 2014;129:e482-e484. doi:[10.1161/CIRCULATIONAHA.113.006891](https://doi.org/10.1161/CIRCULATIONAHA.113.006891)
80. Guo W, Zhu C, Yin Z, et al. Splicing factor RBM20 regulates transcriptional network of Titin associated and calcium handling genes in the heart. *Int J Biol Sci.* 2018;14:369-380. doi:[10.7150/ijbs.24117](https://doi.org/10.7150/ijbs.24117)
81. van den Moogenhof MMG, Beqqali A, Amin AS, et al. RBM20 mutations induce an Arrhythmogenic dilated cardiomyopathy related to disturbed calcium handling. *Circulation.* 2018;138:1330-1342. doi:[10.1161/CIRCULATIONAHA.117.031947](https://doi.org/10.1161/CIRCULATIONAHA.117.031947)
82. Beqqali A, Bollen IAE, Rasmussen TB, et al. A mutation in the glutamate-rich region of RNA-binding motif protein 20 causes dilated cardiomyopathy through missplicing of titin and impaired Frank-Starling mechanism. *Cardiovasc Res.* 2016;112:452-463. doi:[10.1093/cvr/cvw192](https://doi.org/10.1093/cvr/cvw192)
83. Kameda S, Higo S, Shiba M, et al. Modeling reduced contractility and stiffness using iPSC-derived Cardiomyocytes generated from female Becker muscular dystrophy carrier. *JACC: Basic to Translational Science.* 2023;8:599-613. doi:[10.1016/j.jacbts.2022.11.007](https://doi.org/10.1016/j.jacbts.2022.11.007)
84. Buck D, Smith JE III, Chung CS, et al. Removal of immunoglobulin-like domains from titin's spring segment alters titin splicing in mouse skeletal muscle and causes myopathy. *J Gen Physiol.* 2014;143:215-230. doi:[10.1085/jgp.201311129](https://doi.org/10.1085/jgp.201311129)
85. Ma W, Buck D, Nedrud J, Irving T, Granzier H. Thick filament compliance in passively stretched skeletal muscle. *Biophys J.* 2017;112:181a. doi:[10.1016/j.bpj.2016.11.1005](https://doi.org/10.1016/j.bpj.2016.11.1005)
86. Pijl RJVD, Granzier HL, Ottenheijm CAC. Diaphragm contractile weakness due to reduced mechanical loading: role of titin. *Am J Phys Cell Phys.* 2019;317:C167-C176. doi:[10.1152/ajpcell.00509.2018](https://doi.org/10.1152/ajpcell.00509.2018)
87. Papa R, Madia F, Bartolomeo D, et al. Genetic and early clinical manifestations of females heterozygous for Duchenne/Becker muscular dystrophy. *Pediatr Neurol.* 2016;55:58-63. doi:[10.1016/j.pediatrneurol.2015.11.004](https://doi.org/10.1016/j.pediatrneurol.2015.11.004)
88. Kakulas BA. In: Serratrice G, Pouget J, Azulay J-P, eds. *Exercise Intolerance and Muscle Contracture.* Springer; 1999:75-82.
89. Zhu C, Yin Z, Ren J, McCormick RJ, Ford SP, Guo W. RBM20 is an essential factor for thyroid hormone-regulated titin isoform transition. *J Mol Cell Biol.* 2015;7:88-90. doi:[10.1093/jmcb/mjv002](https://doi.org/10.1093/jmcb/mjv002)
90. Guo W, Pleitner JM, Saupe KW, Greaser ML. Pathophysiological defects and transcriptional profiling in the RBM20^{-/-} rat model. *PLoS One.* 2013;8:e84281. doi:[10.1371/journal.pone.0084281](https://doi.org/10.1371/journal.pone.0084281)
91. Perrin JS, Segall LA, Harbour VL, Woodside B, Amir S. The expression of the clock protein PER2 in the limbic forebrain is modulated by the estrous cycle. *Proc Natl Acad Sci USA.* 2006;103:5591-5596. doi:[10.1073/pnas.0601310103](https://doi.org/10.1073/pnas.0601310103)
92. Nakamura TJ, Sellix MT, Menaker M, Block GD. Estrogen directly modulates circadian rhythms of PER2 expression in the uterus. *Am J Physiol Endocrinol Metab.* 2008;295:E1025-E1031. doi:[10.1152/ajpendo.90392.2008](https://doi.org/10.1152/ajpendo.90392.2008)
93. Nakamura TJ, Sellix MT, Kudo T, et al. Influence of the estrous cycle on clock gene expression in reproductive tissues: effects of fluctuating ovarian steroid hormone levels. *Steroids.* 2010;75:203-212. doi:[10.1016/j.steroids.2010.01.007](https://doi.org/10.1016/j.steroids.2010.01.007)
94. van der Pijl EM, van Putten M, Niks EH, Verschuuren JJGM, Aartsma-Rus A, Plomp JJ. Low dystrophin levels are insufficient to normalize the neuromuscular synaptic abnormalities of mdx mice. *Neuromuscul Disord.* 2018;28:427-442. doi:[10.1016/j.nmd.2018.02.013](https://doi.org/10.1016/j.nmd.2018.02.013)
95. Preuß C, von Moers A, Kölbl H, et al. Inflammation-induced fibrosis in skeletal muscle of female carriers of Duchenne muscular dystrophy. *Neuromuscul Disord.* 2019;29:487-496. doi:[10.1016/j.nmd.2019.05.003](https://doi.org/10.1016/j.nmd.2019.05.003)

SUPPORTING INFORMATION

Additional supporting information can be found online in the Supporting Information section at the end of this article.

How to cite this article: Timpani CA, Debrincat D, Kourakis S, et al. Loss of endogenous estrogen alters mitochondrial metabolism and muscle clock-related protein Rbm20 in female *mdx* mice. *The FASEB Journal.* 2024;38:e23718. doi:[10.1096/fj.202400329R](https://doi.org/10.1096/fj.202400329R)